JOURNAL OF PROPULSION AND POWER
Vol. 9, No. 3, May–June 1993

Development of Braided Rope Seals for Hypersonic Engine Applications: Flow Modeling

Rajakkannu Mutharasan*
Drexel University, Philadelphia, Pennsylvania 19104
Bruce M. Steinetz†
NASA Lewis Research Center, Cleveland, Ohio 44135
and
Xiaoming Tao,‡ Guang-Wu Du,‡ and Frank Ko§
Drexel University, Philadelphia, Pennsylvania 19104

A new type of engine seal is being developed to meet the needs of advanced hypersonic engines. A seal braided of emerging high-temperature ceramic fibers comprised of a sheath-core construction has been selected for study based on its low leakage rates. Flexible, low-leakage, high-temperature seals are required to seal the movable engine panels of advanced ramjet-scramjet engines, either preventing potentially dangerous leakage into backside engine cavities or limiting the purge coolant flow rates through the seals. To predict the leakage through these flexible, porous seal structures, new analytical flow models are required. Two such models based on Kozeny-Carman equations are developed herein and are compared to experimental leakage measurements for simulated pressure and seal preload conditions, showing good agreement. The models developed allow prediction of the gas leakage rate as a function of fiber diameter, fiber packing density, gas properties, and pressure drop across the seal. The first model treats the seal as a homogeneous fiber bed. The second model divides the seal into two homogeneous fiber beds identified as the core and the sheath of the seal.

Nomenclature

A_c	=	cross area of seal
A_y	=	yarn cross-sectional area
D_f	=	fiber diameter
g_c	=	gravitational constant
M	=	mass flow rate of gas
M_w	=	molecular weight of gas
N_c	=	number of core yarns
N_s	=	number of sheath yarns
P_i	=	pressure upstream of seal
P_o	=	pressure downstream of seal
R	=	flow resistance of the seal
Re	=	Reynolds number
R_g	=	universal gas constant
T	=	absolute temperature
t, t_1, t_2	=	seal dimensions (see Fig. 4)
u	=	superficial gas velocity
y_0	=	half the clearance between the seal and its housing
ε	=	porosity [see Eqs. (27–29)]
θ	=	braid angle (see Fig. 1)
μ	=	gas viscosity
ρ	=	gas density
ρ_f	=	mass density of fiber
ϕ	=	shape factor, defined in Eq. (4)

Subscripts

c	=	core
e	=	edge
s	=	sheath
sl	=	seal
1, 2, . . . , 7	=	flow paths (see Fig. 4)

Received May 21, 1991; presented as Paper 91-2495 at the AIAA/SAE/ASME 27th Joint Propulsion Conference, Sacramento, CA, June 24–26, 1991; revision received Oct. 15, 1992; accepted for publication Nov. 13, 1992.

*Professor of Chemical Engineering.
†Research Engineer, Structural Dynamics Branch. Member AIAA.
‡Research Associate, Fibrous Materials Research Center.
§Professor of Materials Engineering.

Introduction

RAMJET-SCRAMJET engines require sliding panel seals to prevent combustion gases from leading past the articulating engine panels, similar to articulating panel seals of turbojet two-dimensional converging-diverging nozzles.[1] However, new seals are required for advanced hypersonic engines because of higher thermal loads and the need to seal larger engine sidewall distortions. As a point of comparison, turbojet nozzle seals developed under the augmented deflector exhaust nozzle program[2] used superalloy seals that sealed pressure differentials up to 30 psi, sealed sidewall distortions up to 0.030 in., and were cooled to 1200°F. Hypersonic engine seals, however, are required to operate at higher temperatures (1800–2000°F), seal high pressure differentials (up to 100 psi), and seal larger sidewall distortions (up to 0.150 in.), as described in Ref. 3.

A seal concept that shows promise of meeting these challenging demands is the braided ceramic rope seal being developed at NASA Lewis Research Center. The braided ceramic rope seal structure consists of a high-density uniaxial core structure overbraided with an outer sheath for structural integrity, as shown in Fig. 1. Braided of emerging high-temperature ceramic fibers, this seal shows promise of operating hot and remaining flexible at temperatures up to 2000°F. Early design studies[4] identified important seal design parameters including (1) fiber diameter, 2) yarn bundle size, 3) fiber packing density, and 4) percent core structure for low leakage.

Accompanying the development of these engine seals, NASA is also developing engine seal flow models to predict the seal leakage through these porous seal structures. These seal flow models can be used during the design process in one of two ways: 1) to predict performance losses associated with para-

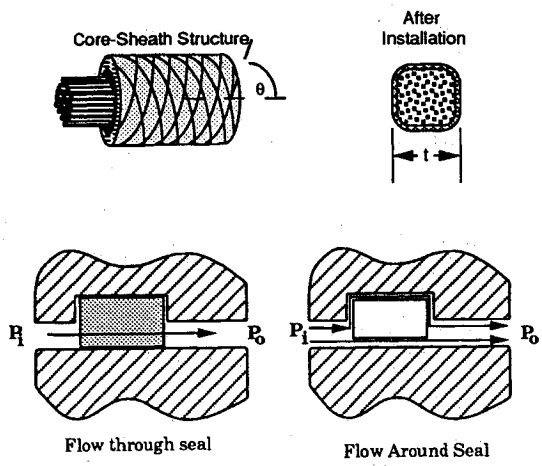

Fig. 1 Definition of seal leakage flow paths.

sitic leakage through the seals; and 2) to predict purge coolant flow rates through these seals where ambient engine flow temperatures exceed the seal's operating temperature limit. The purpose of this article is to provide an analytic means of predicting the gas flow through these braided structures and to determine quantitatively the relationship between gas leakage rate and the pore structure of the seal.

Theoretical

Definition of Flow Path

As shown in Fig. 1, the flow path across a seal system can be divided into two categories: 1) flow through the seal and 2) flow around seal. The flow in the first path is related to the packing architecture of the seal itself, and the flow by way of the second path is dependent on the surface properties of the seal and housing.

Flow Through Seal

Based on data from a large amount of experimental data obtained using a variety of packing materials, both spherical and granular in shape, Ergun[5] derived the following equation:

$$\frac{-(P_o - P_i)g_c}{\rho u^2}\frac{(\phi D)}{t}\frac{\varepsilon^3}{1-\varepsilon} = \frac{150(1-\varepsilon)}{(\delta D)\rho u/\mu} + 1.75 \quad (1)$$

where P denotes pressure, and the subscripts i and o denote the inlet and outlet, respectively. In the above equation, if $Re = (\phi D)\rho u/\mu(1-\varepsilon)$ is small (less than 10), then the constant 1.75 on the right side of the equation can be ignored. In the case of an engine seal, the flow is expected to be laminar as the gas leakage rate and the fiber diameter are small. This implies that the viscous term dominates in the above equation and the inertial term is negligible. Under such a condition, the pressure drop is proportional to u.

In earlier studies, the tortuous pore structure of the bed was modeled as a solid bed consisting of an assembly of capillaries with circular cross section.[6] The capillary model focused on the spaces or the pores in the porous solid. The best known proposed equation based on this approach is the Kozeny-Carman equation,[7] which includes permeability coefficient as a function of porosity. One form of this equation is given below as

$$u = \frac{-(P_o - P_i)g_c}{150[\mu t/(\phi D)^2][(1-\varepsilon)^2/\varepsilon^3]} \quad (2)$$

ϕ is defined as

$$\phi = \frac{\text{area of sphere equivalent to particle volume}}{\text{actual surface area of particle}}$$

ϕ is unity for a sphere and 0.87 for a cylinder with its diameter equal to its length. The equivalent diameter of a particle is defined as the diameter of a sphere having the same volume as the particle. For a fiber with a diameter D_f and length L, the equivalent diameter is

$$D = (1.5D_f^2L)^{1/3} \quad (3)$$

and the shape factor is

$$\phi = (1.5)^{2/3}\frac{(L/D_f)^{2/3}}{L/D_f + 0.5} \quad (4)$$

Therefore, (ϕD) can be expressed as

$$(\phi D) = 1.5D_f\frac{L/D_f}{L/D_f + 0.5} \quad (5)$$

If the ratio L/D_f is very large, the term (ϕD) will approach the value of $1.5D_f$. If the direction of flow is across the axis of fiber (a situation that occurs in a seal containing a substantial amount of longitudinal fibers), the length scale L in the above equation should be expected to be of the same order of magnitude as the diameter of the fiber. The parameter (ϕD) can be thought of as characteristic dimension intrinsic to flow through the fibrous seal.

The Kozeny-Carman equation successfully predicts the pressure drop in packed beds with porosity ranging from 0.3 to 0.6. For porous media with higher porosity, such as most fiber beds and textile fabrics, a number of authors (e.g., see Ref. 8) have shown that predicted pressure drop is much greater than measured values. In the current application, for determining leakage rate of a gas through a seal having low porosity, Kozeny-Carman equation is a good starting point. Taking the cross-sectional area for gas flow as A_c and the seal length as L, Eq. (2) can be rearranged as

$$\frac{\dot{M}}{L} = \frac{-(P_o^2 - P_i^2)}{300(\mu R_gT/M_wg_c)(tL/A_c)[(1-\varepsilon)^2/\varepsilon^3(\phi D)^2]} \quad (6)$$

where ideal behavior of gas is assumed, and ρ is based on an average value evaluated at the two end-point pressures as

$$\rho = [(P_o + P_i)M_w/2R_gT] \quad (7)$$

Flow Around Seal

Edge flow can be treated as a flow between parallel nonporous surfaces separated by a small gap. Assuming that the gap between the surfaces can be considered constant and equal to $2y_0$, one can relate the pressure difference across the seal to the gas leakage velocity as[9]

$$P_o - P_i = (3\mu ut/g_cy_o^2) \quad (8)$$

Rearranging the above in the form of Eq. (6) gives

$$\frac{\dot{M}}{L} = \frac{-(P_o^2 - P_i^2)}{(3\mu R_gT/M_wg_c)(t/y_o^3)} \quad (9)$$

Flow Resistance

Examination of Eq. (6) for flow though the seal and Eq. (9) for flow around the seal suggests the definition of R as

$$R = [-(P_0^2 - P_i^2)/\dot{M}/L] \quad (10)$$

R is a function of properties of both fluid and seal architecture and, for this analysis, is assumed to be independent of the pressure difference across it and any compressive pressure to which the seal may be subjected.

Flow Modeling

In a previous paper,[4] critical design parameters such as fiber packing density and fiber bundle size were identified through a combination of theoretical and experimental studies. Since the seal consists of both braids in the sheath and longitudinal fibers in the core, one expects different porosity values to be applicable in the two regions. In this investigation, two models are proposed to quanitatively evaluate the flow resistances.

Model I

As shown in Fig. 2, the seal is assumed to be a homogeneous fiber bed having a uniform constant porosity regardless of the core and sheath structures. Thus, only one value of porosity is used to calculate the flow resistance. The gas leakage rate can be expressed as the sum of the leakages through the seal and around the seal, and is given by

$$\frac{\dot{M}}{L} = \frac{\dot{M}_e}{L} + \frac{\dot{M}_{sl}}{L} = \frac{(P_i^2 - P_o^2)}{R} \tag{11}$$

The individual leakages are given by

$$\frac{\dot{M}_e}{L} = \frac{(P_i^2 - P_o^2)}{R_e} \tag{12}$$

$$\frac{\dot{M}_{sl}}{L} = \frac{(P_i^2 - P_o^2)}{R_{sl}} \tag{13}$$

The flow resistances encountered in the flow path through the seal are determined from Eq. (6) and are given as

$$R_{sl} = 300\,\frac{\mu R_g T t L (1-\varepsilon)^2}{M_w g_c A_c \varepsilon^3 (\phi D)^2} \tag{14}$$

The edge flow consists of two parallel paths as shown in Fig. 2, and the flow resistance of each of these two paths may be summed in parallel as

$$R_e = \frac{R_{e1} R_{e2}}{R_{e1} + R_{e2}} \tag{15}$$

with

$$R_{e1} = 9\,\frac{\mu R_g T}{M_w g_c}\,\frac{t}{y_o^3}$$

$$R_{e2} = 3\,\frac{\mu R_g T}{M_w g_c}\,\frac{t}{y_o^3}$$

where R_{e1} is three times R_{e2} because of the longer path length (see Fig. 2). Since the edge flow and flow through the seal occur in parallel, the overall flow resistance of the seal system is therefore given by

$$R = [R_e R_{sl}/(R_e + R_{sl})] \tag{16}$$

Model II

The second model, illustrated in Fig. 3, deals with a composite seal in which the sheath and core are allowed to have

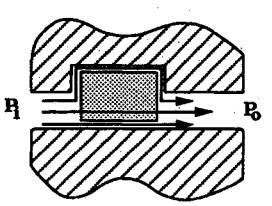

Fig. 2 Schematic diagram for flow model I: uniform seal porosity.

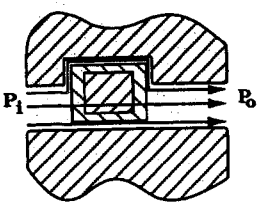

Fig. 3 Schematic diagram for flow model II: independent sheath and core porosities.

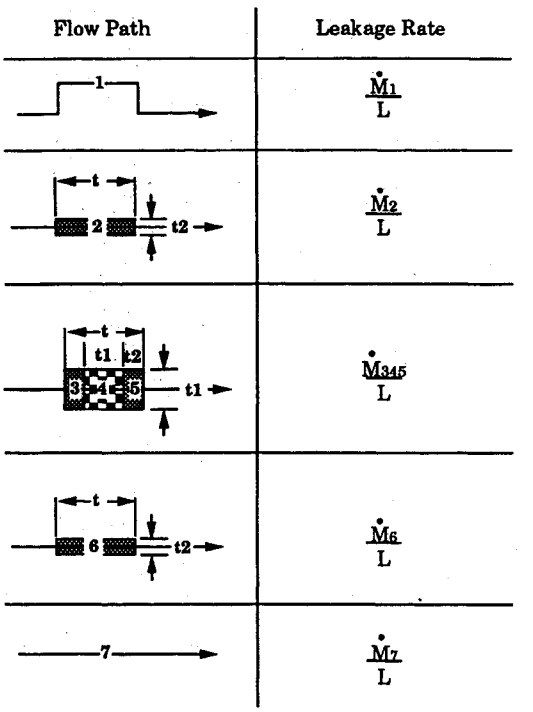

Fig. 4 Flow paths used in calculating total flow resistance for model II.

independent porosity values. The seal has a sheath and a core with porosities ε_s and ε_c, respectively. Flow resistances along the various flow paths illustrated in Fig. 4 are given as

$$R_1 = 9K(t/y_o^3) \tag{17}$$

$$R_2 = R_6 = 300K(t/t_2)[(1-\varepsilon_s)^2/\varepsilon_s^3(\phi D)^2] \tag{18}$$

$$R_3 = R_5 = 300K(t_2/t)[(1-\varepsilon_s)^2/\varepsilon_s^3(\phi D)^2] \tag{19}$$

$$R_4 = 300K[(1-\varepsilon_c)^2/\varepsilon_c^3(\phi D)^2] \tag{20}$$

$$R_{345} = R_3 + R_4 + R_5 \tag{21}$$

$$R_7 = 3K(t/y_o^3) \tag{22}$$

where $K = \mu R_g T/M_w g_c$. The flow resistance of the seal can be determined by summing the flow resistances in parallel, given as

$$(1/R_s) = (1/R_2) + (1/R_{345}) + (1/R_6) \tag{23}$$

Flow resistance of edge flow is

$$R_e = [R_1 R_7/(R_1 + R_7)] \tag{24}$$

The total flow resistance of the seal for substitution into Eq. (11) is then given by

$$R = [R_e R_s/(R_e + R_s)] \tag{25}$$

Calculation Basis

Two important parameters in determining flow resistance through the seal are porosity and the characteristic dimension D. The actual porosity of the seal in the application condition is expected to be lower than in the initial installed position. The porosity (method of determination discussed below) was assumed to be a constant for any given seal. With regard to D, since the bulk of the seal is made up of longitudinal fibers and the number of fiber-fiber interfaces is significantly larger than the number of yarn-yarn interfaces, the characteristic dimension was taken as D_f. The characteristic dimension (ϕD) takes on values between $1.5D_f$ and $0.75D_f$ when the ratio L/D_f is taken to be large or 0.5, respectively. The latter value gives a better fit with experimental data under a variety of situations investigated. Therefore, all calculations presented in this article are based on $(\phi D) = 0.75D_f$.

Another characteristic dimension is the distance y_o in calculating seal edge leakage. In the present calculation, the clearance was assumed to be proportional to fiber diameter. Specifically y_o is assumed to be $0.1(\phi D)$.

A_y (in.^{2}) can be determined from its denier and fiber density ρ_f(g/cm^3) as

$$A_y = \frac{\text{yarn denier}}{5.8 \times 10^6 \rho_f} \tag{26}$$

where denier is a yarn density term used in the textile industry and is the yarn mass in grams per 9000 m of length.

The following are the parameters used for calculation of various results reported:

ρ_f	= 2.54 g/cm^3
R_g	= 1.545 × 10^3 lb-ft/°R
T	= 528°R
g_c	= 32.1 lb$_m$ ft/lb$_f$ s^2
D_f	= 10 μm
denier	= 812 g per 9000 m
(ϕD)	= $0.75D_f$
y_o	= $0.1(\phi D)$
M_w (air)	= 29 lb$_m$/lb mole
M_w (He)	= 4 lb$_m$/lb mole
μ of air	= 0.0175 cP
μ of helium	= 0.019 cP

Experimental

Braided Seal Specimens

Eight seal specimens were made using 812 denier E-glass fibers (Owens Corning Glass, Granville, Ohio). The specimens were labels A1 through H1 and their architectural parameters, braiding angle, number of longitudinal yarns, and number of braiding yarns are summarized in Table 1. Specimens G1 and H1 have the highest number of longitudinal yarns, whereas A1, B1, and C1 have the lowest number of longitudinal yarns. For engine applications, ceramic fibers are substituted in place of E-glass fibers. Comparable diameter E-glass fibers were immediately available, and therefore, were used for these early braid/flow studies.

Flow Measurement

The experimental details of the flow measurement were described in an earlier paper by the authors.[4] Seal specimens 1 ft in length were mounted in a specially developed test fixture, and were leak tested under room temperature at various inlet pressure conditions in the range of 5–80 psig. The pressure upstream of the seal was varied and the resulting leakage of gas (either air or helium) was measured. Lateral preloads were applied uniformly to the back of the seal with an inflatable rubber diaphragm at either 80 or 130 psig. The flow resistance of the seal was computed from the ratio of the difference of squares of absolute pressures over the mass leakage rate.

Porosity

An ultralow viscosity embedding media (purchased from Polysciences Inc., Warrington, PA) was used as a rigidizing medium to infiltrate the specimen. Polymerization was accomplished at 70°C for 12 h. The specimen then was cut and polished. Scanning electron micrographs were taken to determine the dimension of the seal cross section and packing geometry of fibers. The thickness of the braid sheath, t_2, was measured using the electron photomicrographs.

Porosity of the seal for calculating flow resistances described earlier was obtained from the geometry of fiber layout and is given by

$$\varepsilon = 1 - [A_y(N_c + N_s/\cos\theta)/t^2] \tag{27}$$

where N_c and N_s are the number of core and sheath yarns, and t^2 is the cross-sectional area of the installed seal. Note that the seal is treated as a homogeneous fiber bed having a single average porosity value for model I.

The porosity of sheath and core sections of the specimens for model II were determined from the following two equations:

$$\varepsilon_c = 1 - (A_y N_c/t_1^2) \tag{28}$$

$$\varepsilon_s = 1 - [A_y N_s/\cos\theta/(t^2 - t_1^2)] \tag{29}$$

where t and t_1 are the overall width of the installed seal, and the width of the core region, respectively (see Fig. 4).

Results and Discussion

Pressure Drop Correlations

In Fig. 5, typical measured air leakage rates are plotted as a function of the difference of the squares of the pressure across the seal for specimens A1 and G1 at preload pressures of 80 and 130 psig. The linear relationship between the two variables is indicative of the validity of the pressure dependency presented earlier in Eq. (10). Although only two sample

Table 1 Seal construction details and porosity data

Sample number	Braiding angle, θ, deg	Core fiber, %	Average porosity[a]	Thickness t_2[d]	Core porosity[b]	Sheath porosity[c]
A1	45	39.6	0.48	0.11	0.34 ± 0.04	0.54 ± 0.02
B1	30	39.4	0.48	0.12	0.24 ± 0.06	0.56 ± 0.01
C1	10	41.1	0.50	0.09	0.50 ± 0.03	0.50 ± 0.02
D1	45	57.2	0.42	0.09	0.19 ± 0.05	0.58 ± 0.02
E1[e]	30	60.7	0.46	n/a	n/a	n/a
F1[e]	10	55.0	0.40	n/a	n/a	n/a
G1	45	82.2	0.45	0.02	0.47 ± 0.02	0.37 ± 0.16
H1	30	81.3	0.45	0.02	0.47 ± 0.02	0.32 ± 0.18

[a]Calculated from Eq. (27). [b]Calculated from Eq. (28). [c]Calculated from Eq. (29). [d]The accuracy of t_2 measurement was in the range of ±0.005. [e]E1 and F1 were damaged during use.

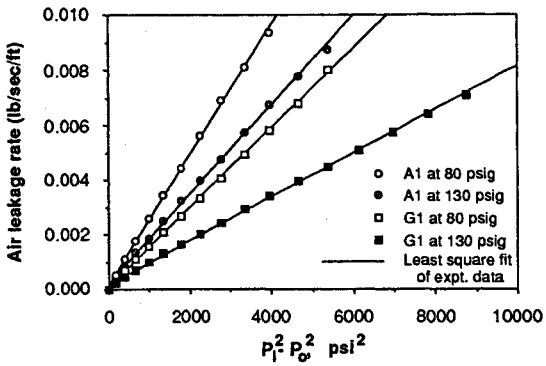

Fig. 5 Measured seal leakage data validating seal leakage pressure dependence.

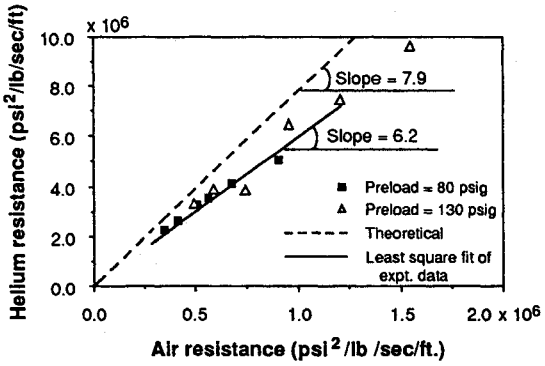

Fig. 6 Measured seal flow resistances of air and helium compared to theoretical expectations.

results are shown in Fig. 5, all eight specimens examined in this investigation showed excellent correlation with correlation coefficient lying in the range of 0.990–0.999. The slope of the line in Fig. 5 is equal to the inverse of flow resistance, $1/R$.

Flow Resistances for Different Gases

Because of the many environments the seals are expected to operate in, it is important to be able to predict the flow resistance to various potential coolants or leakage gases. Shown in Fig. 6 is the measured resistance of helium plotted against the resistance of air for a wide range of seal architectures (specimens A1, B1, C1, D1, G1, and H1), pressure drop conditions (between 5–80 psig), and preload conditions (80 and 130 psig) investigated. If the seal's pore structure is constant, flow resistance is directly proportional to viscosity and inversely proportional to density of the flowing gas [e.g., Eq. (6)]. Hence, when we compare the flow resistance of helium to that of air in Fig. 6, we expect the slope of the straight line to be

$$\text{SLOPE} = [(\mu/M_w)_{\text{Helium}}/(\mu/M_w)_{\text{Air}}] \qquad (30)$$

The straight line indicated in Fig. 6 is the theoretical line with a slope of 7.9 obtained using Eq. (30). Experimental data given in Fig. 6 when fitted with a straight line yielded a slope of 6.2, which is slightly lower than the theoretical value of 7.9.

Comparison of Measured and Predicted Leakage Rates

The measured and predicted leakage rates for A1 and G1 seals with widely different seal architectures are shown in Figs. 7 and 8 for applied pressure differentials up to 80 psi for both air and helium test gases. Also shown in the figures are the effects of lateral preload on seal leakage. Lateral preloads of 80 and 130 psig were applied to the back of the seal with a diaphragm compressing the seal against the adjacent sidewall.

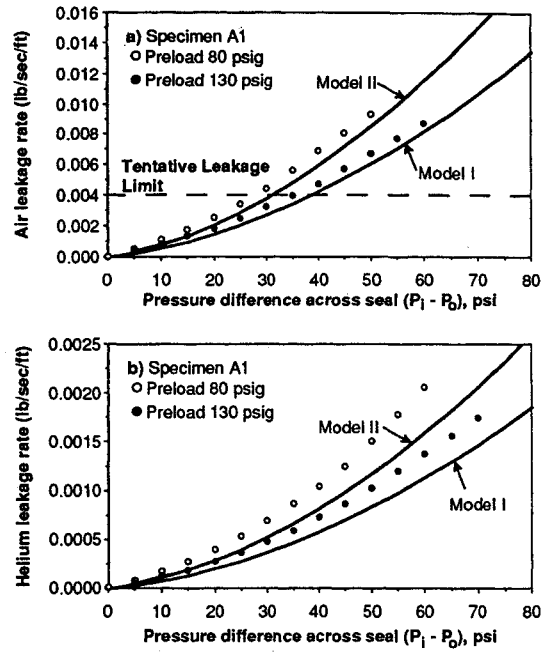

Fig. 7 Seal A1: Measured leakage rates vs pressure drop (symbols) compared to predictions (lines): a) air and b) helium.

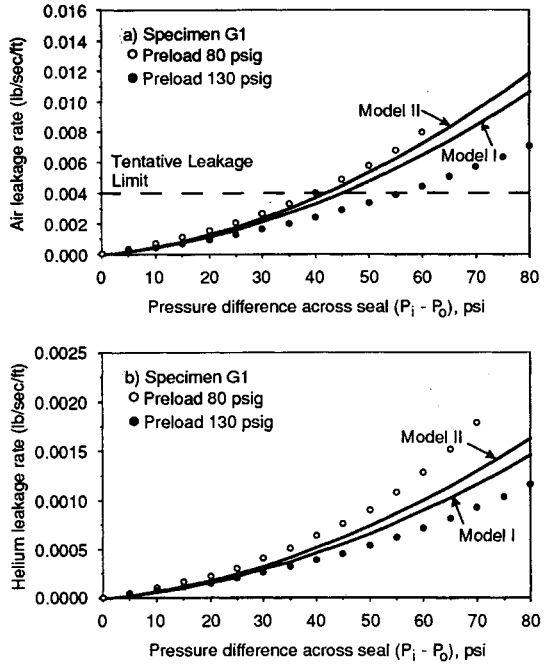

Fig. 8 Seal G1: Measured leakage rates vs pressure drop (symbols) compared to predictions (lines): a) air and b) helium.

Key braiding and geometry parameters of these two seal structures, denoted A1 and G1, are listed in Table 1.

Comparing the overall leakage rates between specimen A1 and G1 finds that the leakage rates for G1 are considerably less than A1. Specimen G1 meets the tentative leakage limit of 0.004 lb/s/ft (e.g., Ref. 3) for air pressure differentials up to 40 psi with a preload of 80 psig. Specimen A1 meets the leakage limit for pressure differentials only up to 30 psi.

In general, both models predict the leakage rates reasonably well with the measured data over the full pressure range for both air and helium test gases. Model II gives values closer to those measured at a preload of 80 psig, and model I predicts values closer to those measured at 130 psig.

In examining Figs. 7a and 8a, the versatility of model II in predicting actual leakage rates is demonstrated. At a pressure differential of 40 psi and preload of 80 psig, the discrepancy

between the measured and predicted leakage rates were only between 6–13%, even though the overall leakage rates differed by a factor of 1.7.

In all the cases, the fiber diameter was used as the basis of calculation. However, if yarn diameter is used as the equivalent diameter, the prediction of the gas leakage rate is very poor as it differs from experimental observation by more than four orders of magnitudes.

Potential Sources of Modeling Discrepancy

A potential source of the discrepancy between the measured and predicted leakage rates is the porosity dependence on preload. As the preload pressure is increased, the fibers are urged closer to one another and the adjacent surface, making it more difficult for the air to flow around the fibers, thus increasing flow resistance. Neither of the models considered in this article account for this porosity-load dependence, and is presently under development.

The choice of ϕ has a considerable effect on the predicted leakage rates. For example, because in Eq. (6) the term containing (ϕD) is squared, increasing it from $0.75D_f$ to $0.80D_f$ increases the predicted leakage by 14%. Selection of ϕ is based on the quality of the model fit to experimental observations and the seal porosity value used. As improved measured values of porosity become available, it is expected that the shape factor could change and approach the theoretical upper limit of 1.5.

Summary and Conclusions

Two analytical models have been developed for predicting leakage rates of braided rope seals being developed for panels of advanced hypersonic engines. Both models are based on the Kozeny-Carman relations for flow through porous media, where the characteristic size dimension is a scaled fiber diameter (e.g., $0.75D_f$) based on experimental observations.

The first model treats the seal as a homogeneous fiber bed having a single average value for its porosity. The second model treats the two-dimensional braided seal structures as a system of flow resistances analogous to a series of resistors in an electrical network.

Based on the findings from the comparison between measured and predicted leakage rates, the following results were obtained:

1) Leakage rates predicted using model II agree favorably to the measured leakage rates for modest preloads (80 psig) for a wide range of braided seal architectures. Agreement within 6–13% was observed at a pressure differential of 40 psi for seal specimens A1 and G1 whose overall leakage rates differed by a factor of 1.7.

2) Theoretical predictions compared to experimental observations for air and helium indicate that relative resistance to leakage flow depends on the ratio of the quotients of each gas's viscosity and molecular weight.

Acknowledgments

The financial sponsorship of this project from NASA Grant NAG3-1059 is gratefully acknowledged. The authors wish to thank Susan Marr for making most of the specimens.

References

[1]Kuchar, A. D., "Variable Convergent-Divergent Exhaust Nozzle Aerodynamics," *Aircraft Propulsion Systems Technology and Design*, edited by G. C. Oates, AIAA, Washington, DC, 1989, pp. 301–338.

[2]Anon., "Advanced V/STOL Propulsion Component Development. Vol. 1: Nozzle/Deflector. Final Report," Aircraft Engine Group, General Electric Co., R77AEG441-VOL. 1, Cincinnati, OH, Aug. 1977.

[3]Steinetz, B. M., "Evaluation of an Innovative High Temperature Ceramic Wafer Seal for Hypersonic Engine Applications," NASA TM-105556, Feb. 1992.

[4]Ko, F., Steinetz, B. M., and Mutharasan, R., "Development of Braided Rope Engine Seals," NASA TM-105902, 1993.

[5]Ergun, S., "Fluid Flow Through Packed Columns," *Chemical Engineering Progress*, Vol. 48, No. 2, 1952, pp. 89–94.

[6]White, F. M., *Viscous Fluid Flow*, McGraw-Hill, New York, 1974.

[7]Scheidegger, A. E., *The Physics of Flow Through Porous Media*, Rev. ed., Univ. of Toronto Press, Toronto, 1960.

[8]Van Den Brekel, L. D. M., and De Jong, E. J., "Hydrodynamics in Packed Textile Beds," *Textile Research Journal*, Vol. 59, No. 8, 1989, pp. 433–440.

[9]Bennett, C. O., and Myers, J. E., *Momentum, Heat and Mass Transfer*, 3rd ed., McGraw-Hill, New York, 1982.